Electrochemiluminescent Arrays for Toxicity Screening

by James F. Rusling

Electrochemical applications to biomedical problems began in the early days of quantitative polarography and this topic was reviewed in a classic book by Březina and Zuman published over 50 years ago.[1] In recent years, commercial electrochemical enzyme sensors have become the method of choice for diabetic patients to measure glucose in their blood,[2] and a myriad of electrochemical sensors have been developed to detect other biomolecules including DNA for genetic analysis and protein biomarkers for disease detection and monitoring. Advantages such as low cost and mobility of instrumentation, and simplicity of procedures promise to lead to eventual medical point-of-care applications.

Electrochemiluminescence as a Detection Method

The electrochemically driven light-producing technique electrochemiluminescence (ECL) has grown in importance as a detection method for many types of bioanalysis.[3,4] In a typical scenario, tris (2,2′-bipyridyl)ruthenium(II), ($[Ru(bpy)_3]^{2+}$, or RuBPY) produces ECL in connection with a suitable sacrificial reductant such at tripropylamine (TprA). The mechanism of light production is somewhat complex[5] as illustrated in Scheme 1. In essence, TprA oxidized at an electrode produces TprA• (Eq. 1 & 2), which reduces $[Ru(bpy)_3]^{2+}$ to $[Ru(bpy)_3]^{+}$ (Eq. 3). The latter is oxidized by TprA•⁺ to a photoexcited species that emits at 610 nm (Eq. 5). The light can be measured with a photomultiplier tube or a CCD camera. This pathway of ECL generation has been used with RuBPY labels for detection of DNA and proteins.[3] Magnetic bead-based methods have been the most successful in this respect, and have been commercialized.[6,7] For example, in the Roche Diagnostics ELECSYS immunoassay for prostate specific antigen (PSA), capture-antibody-coated magnetic beads are mixed with the sample and bind PSA. Then, a secondary monoclonal PSA-specific antibody labeled with $[Ru(bpy)_3]^{2+}$ is added to bind to the PSA on the beads. After washing to remove non-specific binding, the beads are conveyed to a measuring cell where the microparticles are attracted magnetically onto an electrode for ECL measurement.[7]

In 2003, in collaboration with Lynn Dennany and Robert Forster[8] we found that the metallopolymer (bis-2,2′-bipyridyl) ruthenium polyvinylpyridine ($[Ru(bpy)_2(PVP)_{10}]^{2+}$ or Ru-PVP) reacts electrocatalytically with DNA in thin films to produce visible light by ECL. Damaged DNA, such as occurs when DNA reacts with drug metabolites, gave more light than intact double stranded (ds) DNA. This discovery opened the door to reagentless biosensors and arrays for toxicity screening. The reaction pathway (Scheme 2) has similarities to Scheme 1, except that Ru^{II}-PVP is directly oxidized at the electrode, and guanine moieties in the DNA act as the sacrificial reductants.

Chemical Toxicity Screening

Before proceeding to a description of ECL toxicity screening arrays, we first explain how the measurement of DNA damage is used as an endpoint for chemical toxicity screening. The importance of this problem is highlighted by the experience of the pharmaceutical industry, where 30% of drug development failures are linked to toxicity that is undetected until clinical trials or even after the drug is marketed. Thus, predicting toxicity at the earliest stages of drug development has become a critical issue.[9]

Strategies employed for early toxicity prediction usually involve a range of *in vitro* and *in vivo* bioassays.[9-11] Several years ago, we perceived an unfilled niche for simple, cheap, high throughput, biochemically-based screening assays that can be arranged into array formats that were concurrently emerging.[12,13] Inexpensive toxicity arrays of this sort complement existing *in vitro* toxicity bioassays and can be used at very early stages of drug development to contribute information about chemical toxicity for screening decisions.

Reactions of DNA with chemicals or more frequently with their enzyme-generated metabolites can produce covalently linked nucleobase adducts that often initiate cancer.[14-16] These adducts most often occur on guanine and adenine bases in DNA, and serve as good biomarkers for cancer risk. They are convenient biomarkers for detecting the reactive metabolites and thus for predicting drug toxicity.[13] *Bioactivation* is the term used to denote generation of reactive metabolites by cytochrome P450s (cyt P450) and other metabolic enzymes, leading to what is called genotoxicity. Many organic molecules yield DNA-reactive metabolites, including styrene, benzo[a]pyrene, nitrosamines, napthylamines, and tamoxifen and other therapeutic agents.[17-21] These reactive species can also damage proteins and other biomolecules. Cyt P450s are iron-heme enzymes (P-Fe) that catalyze the transfer of oxygen atoms to organic substrates.[22,23] Oxidations catalyzed by human liver cyt P450s are a major source of reactive metabolites of foreign lipophilic molecules. Other metabolic catalysts called bioconjugation enzymes add chemical groups to molecules and account for ~25% of marketed drug metabolism, Bioconjugation enzymes can contribute to bioactivation alone or in sequential reactions with cyt P450s.[24]

Toxicity Screening with ECL Arrays

The ECL arrays described below detect DNA damage from metabolites as a genotoxicity endpoint. They contain DNA, the Ru-PVP polymer, and sources of metabolic enzymes in spots produced by layer-by-layer (LbL) deposition.[25,26]

Scheme 1. Pathway for ECL generation using TprA as reductant.

$$TPrA \rightarrow TPrA^{\bullet +} + e^- \quad (1)$$

$$TPrA^{\bullet +} \rightarrow TPrA^{\bullet} + H^+ \quad (2)$$

$$TPrA^{\bullet} + [[Ru(bpy)_3]^{2+}] \rightarrow [Ru(bpy)_3]^{+} + \text{products} \quad (3)$$

$$[Ru(bpy)_3]^{+} + TPrA^{\bullet +} \rightarrow [[Ru(bpy)_3]^{2+}]^{*} + \text{products} \quad (4)$$

$$[[Ru(bpy)_3]^{2+}]^{*} \rightarrow [Ru(bpy)_3]^{2+} + h\nu\ (610\ nm) \quad (5)$$

Scheme 2. Pathway for ECL using DNA as reductant, G = guanine moiety.

$$Ru^{II}\text{-PVP} \leftrightarrow Ru^{III}\text{-PVP} + e^- \text{ (at electrode)} \quad (6)$$

$$Ru^{III}\text{-PVP} + G \rightarrow Ru^{II}\text{-PVP} + G^{\bullet} + H^+ \text{ (\textit{rds, faster rate = larger signal})} \quad (7)$$

$$G^{\bullet} + Ru^{III}\text{-PVP} \rightarrow G_{2ox} + Ru^{II*}\text{-PVP (light emitting species)} \quad (8)$$

or:

$$G^{\bullet} + Ru^{II}\text{-PVP} \rightarrow G_{2ox} + Ru^{I}\text{-PVP; then } Ru^{II}\text{-PVP} + Ru^{I}\text{-PVP} \rightarrow Ru^{II*}\text{-PVP} \quad (9)$$

$$Ru^{II*}\text{-PVP} \rightarrow Ru^{II}\text{-PVP} + h\nu \rightarrow (610\ nm) \quad (10)$$

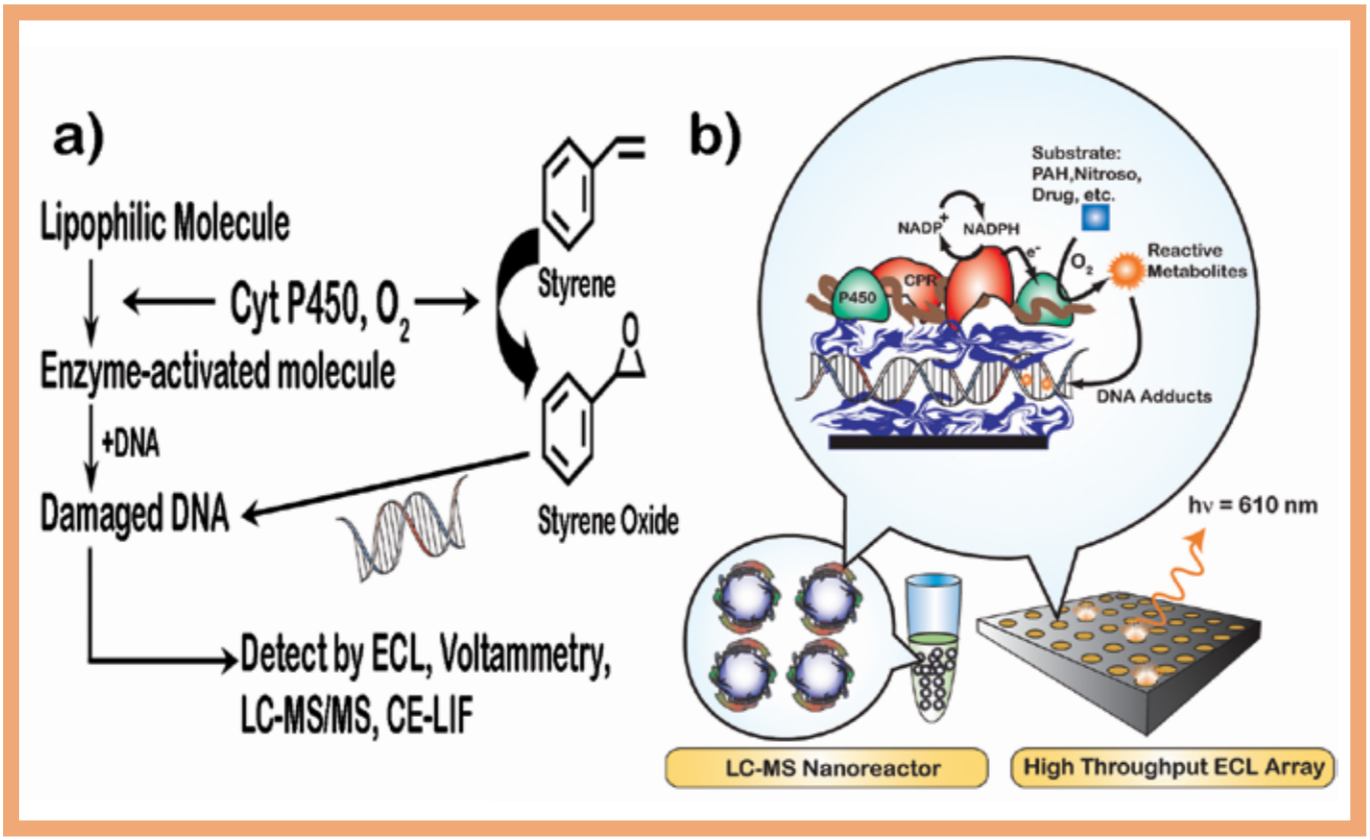

Fig. 1. *Strategies for metabolic toxicity screening. (a) The chemistry: reactive metabolite styrene oxide is formed by cyt P450 enzyme and oxygen, then the epoxide reacts with DNA damage as a endpoint that can be measured by ECL arrays and other approaches. (b) Microsome/DNA films used in enzyme/DNA nanoreactors (left) or ECL array chip; (right): A layer of cationic Ru-PVP polymer is initially deposited (blue ribbon in circle) followed by layers of negative DNA, polycation, and microsomes as a source of enzymes (membrane is brown, cyt P450 reductase (CPR) = red, and cyt P450 = green; (PEI = polyethyleneimine; RuPVP = $[Ru(bpy)_2PVP_{10}]^{2+}$; bpy = bipyridine). In the first step, NADPH generated by an enzyme reaction in solution reduces CPR, which transfers electrons to cyt P450s. O_2 and cyt P450 combine to convert substrate to reactive metabolites that form DNA adducts in the film. In the second step, ECL from the array is detected with a CCD camera upon application of +1.25 V vs. Ag/AgCl and monitors DNA adduct accumulation. Hydrolysis can be used to release labile DNA adducts from the nanoreactor particles for LC-MS analysis to obtain direct structural and formation rate confirmation of the ECL array results.*

The enzyme reaction is run first, then ECL is use to measure the rate of DNA damage. The strategy used is illustrated by Fig. 1.

Our first ECL toxicity sensors employed a pyrolytic graphite electrode coated with DNA, Ru-PVP and metabolic enzymes and interfaced with a photomultiplier tube (Fig. 2A).[27] Later an array format was developed (Fig. 2B).[28] The first two steps in the reactive metabolite detection pathway (Scheme 2) are the same as in electrocatalytic oxidation of DNA by soluble $Ru(bpy)_3^{2+}$ as elucidated by Thorp.[29] Equation 7 is the rate-determining step (*rds*) and the ECL signal increases as this reaction becomes faster. Damaged DNA gives larger signals than intact ds-DNA because as adducts form on bases the DNA double helix unravels. Guanines in the partly unraveled double strands become more available to the Ru-PVP catalyst, increasing rates of the *rds* step in Eq. 7 and increasing ECL.[8] Thus, DNA damage can be used as an endpoint for genotoxicity with ECL detection monitoring the formation of reactive metabolites trapped by DNA, as illustrated for styrene oxide in Fig. 1. When styrene is oxidized to styrene oxide

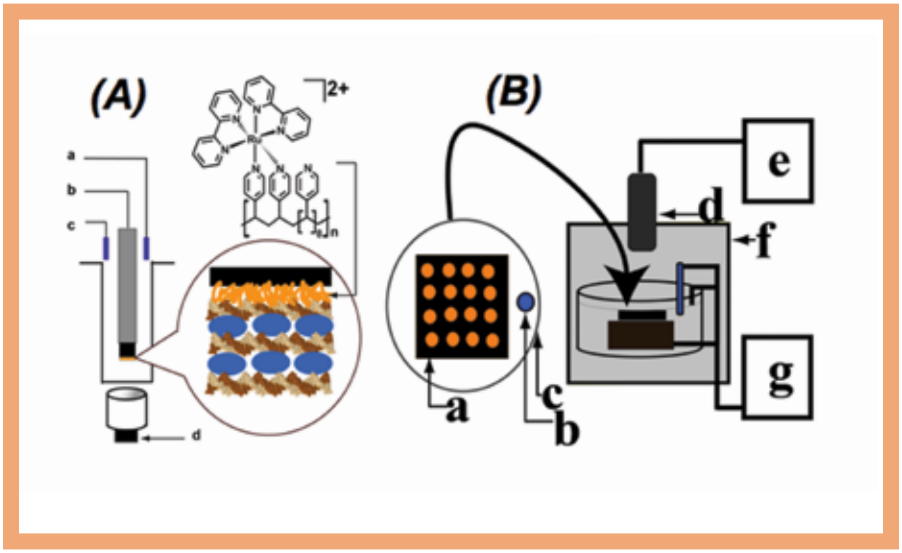

Fig. 2. *Two configurations for ECL detection of metabolite-based DNA damage: (A) sensor for simultaneous ECL detection and voltammetry showing (a) reference, (b) sensor, and (c) counter electrodes located in a glass cell with a cylindrical base. Fiber optic (d) is outside the cell directly under the sensor leading to a photomultiplier tube. Ru-PVP (top structure), DNA (brown), and enzyme (blue) layers form active sensor film shown on right. (B) ECL arrays featuring: (a) array, (b) reference electrode, (c) counter electrode, (d) CCD camera, (e) computer, (f) dark box, and (g) potentiostat to apply voltage. Active enzyme/DNA/Ru-PVP films are 20-40 nm thick. In the first operational step, the enzyme in the film converts substrates to reactive metabolites in close proximity to DNA. Resulting damage to DNA from these reactive metabolites is detected in the second operational step by ECL at an applied voltage 1.25 V for 20 s.[28]*

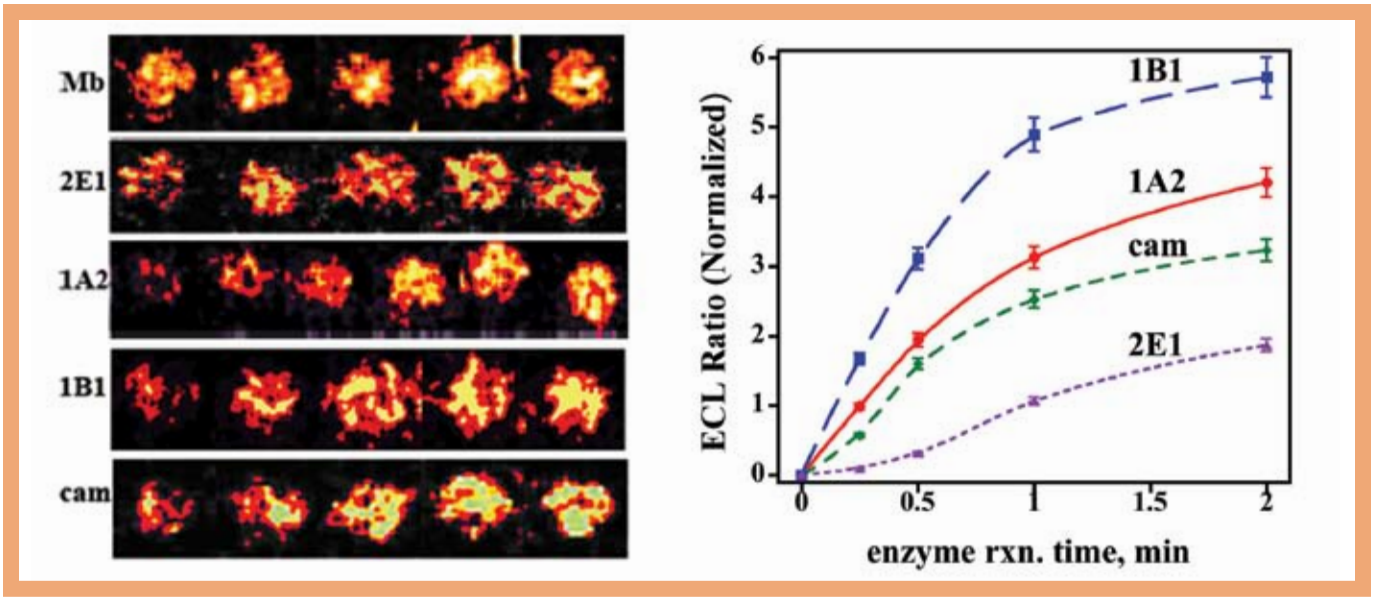

Fig. 3. *ECL array results for enzyme reactions with 100 μM benzo[a]pyrene + 0.5 mM H_2O_2 (a) reconstructed images for different reaction times (0, 1, 3, 5, 7 min) for cyt P450 enzymes and myoglobin on the same array. Brighter spots indicated more DNA damage. (b) ECL initial/final ratios normalized for the amount of enzyme in each spot estimated by quartz crystal microbalance studies. Adapted with permission from Ref. 28, copyright 2007 American Chemical Society.*

by cyt P450 enzymes in the presence of DNA, guanine and adenines in DNA form covalent adducts, and will increase ECL in the array measurement step.

ECL detection facilitates arrays that can be spotted directly onto a single conductive chip, *e.g.* a small pyrolytic graphite (PG) block, thus avoiding the need for individually addressable electrodes. Our high throughput toxicity screening arrays are based on multiple spots of DNA, enzyme and the Ru-PVP polymer (Figs. 1 and 2). Up to 50 individual spots, each an LbL film containing DNA, enzyme and Ru-PVP, can be manually micropipetted onto the 1 x 1 inch PG array chip.[28] Automated spotting devices can be used to deposit hundreds of spots on similar PG chips.

The metabolic enzyme reaction is run first by providing the array with a solution containing enzyme activating factors and oxygen. The array is then washed and placed into an electrochemical cell filled with electrolyte solution and housed in a dark box with a CCD camera (Fig. 2B).[28] Application of 1.25 V vs. SCE causes electrochemical oxidation of Ru-PVP initiating the ECL generation pathway in Scheme 2 and providing light from each spot. The light is measured with the CCD camera over an integration time of ~20 s. As mentioned previously, larger ECL signals are obtained from damaged DNA because of better accessibility of the guanines to the Ru-PVP catalyst as the ds-DNA unravels due to reactions with metabolites.

The ECL toxicity screening arrays can be configured to measure the time course of reactions catalyzed by a single enzyme, or can contain a collection of enzymes for simultaneous comparison of reactive intermediate formation kinetics. Results can be re-organized and presented in a number of ways by computer software. Figure 3 illustrates oxidation of benzo[a]pyrene (B[a]P) with 5 pure enzymes in a single array activated by hydrogen peroxide.[28] The array data have been rearranged by computer software so that representative spots for a single enzyme lie in each row. Relative rates of DNA damage were estimated simultaneously in this way for the 5 enzymes in ~1 min of enzyme reaction time and 20 s of ECL development time. The slope of the linear ECL increase vs. reaction time correlates with DNA damage rates, and the order of enzyme activity of the cyt P450s was 1B1>1A2>cam>2E1, the same as reported relative activities for B[a]P oxidation.[28] The human cyt P450 1B1 and 2E1 enzymes are the most active. This illustrates the use of the arrays to identify the most active enzyme in producing genotoxic metabolites from B[a]P. Structures of the nucleobase adducts and their formation rates were confirmed by using the DNA/enzyme nanoreactors and LC-MS analysis.[28]

Liver microsomes can also be used in the array spots as convenient sources of multiple metabolic enzymes,[30] as illustrated in Fig. 1B. The advantage here is that the microsomes also contain cyt P450 reductase and the natural enzyme activation process can be used by adding NADPH and an NADPH regeneration enzyme. In addition, time consuming enzyme purification is avoided. Figure 4 shows reconstructed ECL array data for multiple enzyme rat liver microsomes (RLM) and single human enzyme cyt P450 2E1 (h2E1) microsome film spots (including DNA and Ru-PVP) exposed to several substrates and NADPH for various times, along with controls. These data compare relative DNA damage rates from metabolites of the N-nitroso compounds 4-(methylnitrosoamino)-1-(3-pyridyl)-1-butanone (NNK), N-nitrosopiperidine (NPIP), N-nitrosopyrrolidine (NPYR) (Scheme 3) and styrene. ECL from array spots exposed to N-nitroso substrates increased more rapidly with reaction time than those exposed to styrene, suggesting higher reactivity of the N-nitroso metabolites with DNA.

Figure 5 shows the percent (%) ECL increase for each of the exposed substrates from RLM (a) and h2E1 (b) spots processed from the raw array data.[30] The ECL increase is presented relative to the amount of ECL produced from the 0 s spots and corrected for background ECL from a non-exposed control. The spots containing h2E1 generate more ECL (Fig. 5b), indicative of both NNK and NPYR reaction rates with cyt P450 2E1 and an increased amount of enzyme on the array spot based on quartz crystal microbalance (QCM) measurements. Initial slopes of plots in Fig. 5 reflect the relative rate of DNA damage elicited by each substrate as shown by correlation with rates of formation of major guanine adducts measured directly by LC-MS. The ECL slopes measure the relative enzyme turnover rates for conversion of each compound into DNA-reactive metabolites. Each N-nitroso compound showed similar ECL vs. reaction time slopes while styrene demonstrated a much smaller ECL increase over the same time range. The array responses and LC measured adduct formation rates correlated well with *in vivo* rat liver

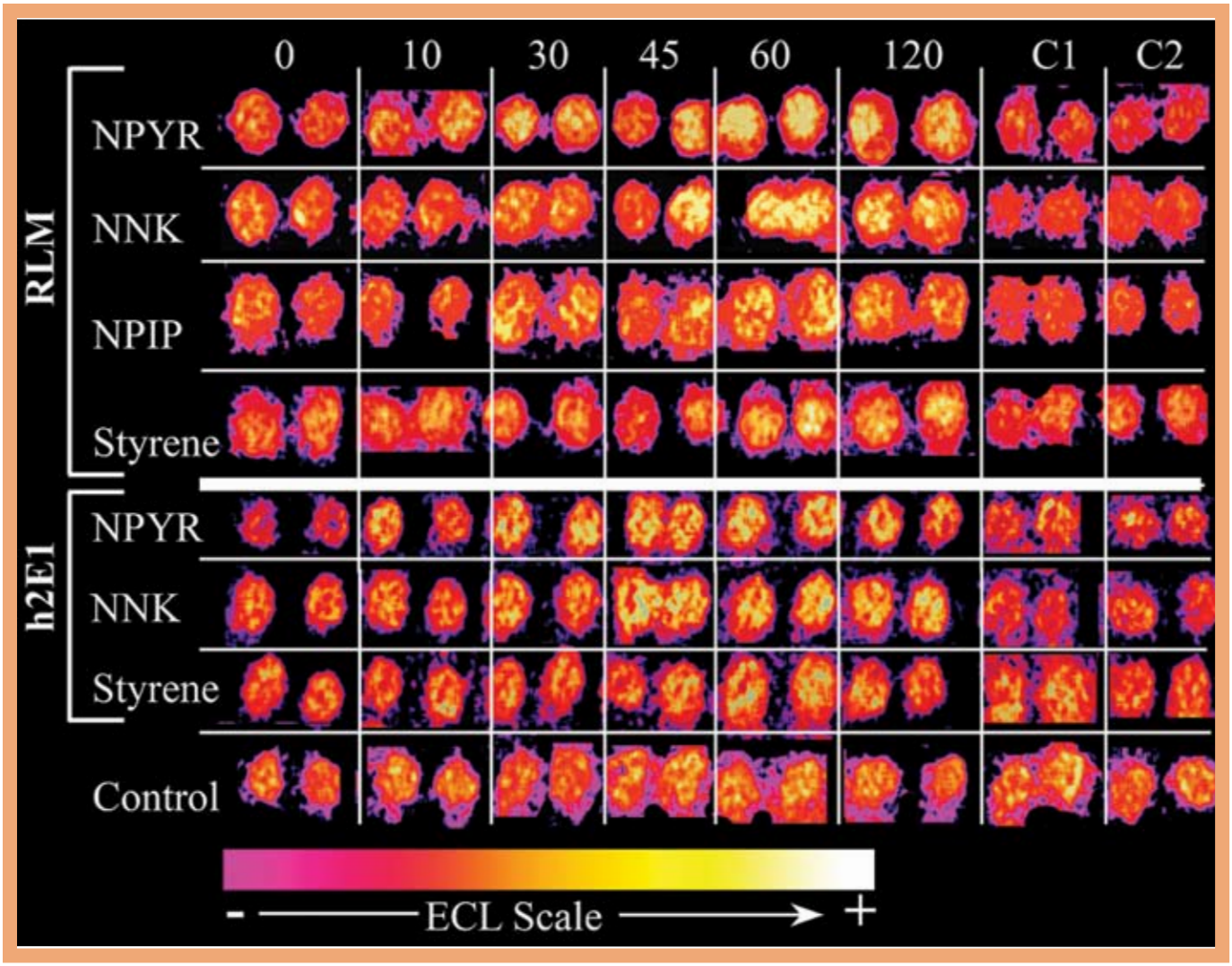

Fig. 4. *Reconstructed array data demonstrating ECL from spots of RuPVP/DNA/RLM (labeled RLM) or RuPVP/DNA/h2E1 (labeled h2E1) exposed to 1 mM of denoted substrate using enzymatic NADPH regeneration for denoted time in sec. Data for respective substrates are from same array run. Control is an identical array (RLM; h2E1 was similar (not shown)) not exposed to reaction solutions. Internal controls C1 = 120 s exposure to NADPH solution only; C2 = 120 s exposure to substrate (no NADPH) only. Substrates: 4-(methylnitrosoamino)-1-(3-pyridyl)-1-butanone (NNK), N-nitrosopiperidine (NPIP), and N-nitrosopyrrolidine (NPYR). Adapted with permission from Ref. 30, copyright 2008 American Chemical Society.*

genotoxicity metrics[30] showing that N-nitroso compounds were much more genotoxic than styrene.

We have also shown that ECL arrays can be used to investigate metabolic inhibition,[30] which is another important measurement impacting drug toxicity. For example, for patient taking two drugs, if Drug 1 inhibits the enzyme that metabolizes Drug 2, concentrations of the latter could become dangerously elevated. We are currently extending the ECL arrays to encompass bioconjugation enzymes and sequential enzyme reactions, which are essential to achieve a representative metabolic toxicity screening array. Our most detailed study involving bioconjugation enzymes so far compared rat liver vs. human liver microsomal (HLM) enzymes in the metabolism of the anti-breast cancer drug Tamoxifen.[31] An approximate two-fold larger DNA damage rate was observed for spots with RLM enzymes compared to HLM enzyme. Utilizing a known tamoxifen metabolic bioconjugation, we activated the enzyme glucuronyl

Scheme 3.N-Nitrosopyrrolidine (NPYR) metabolism leading to DNA damage.

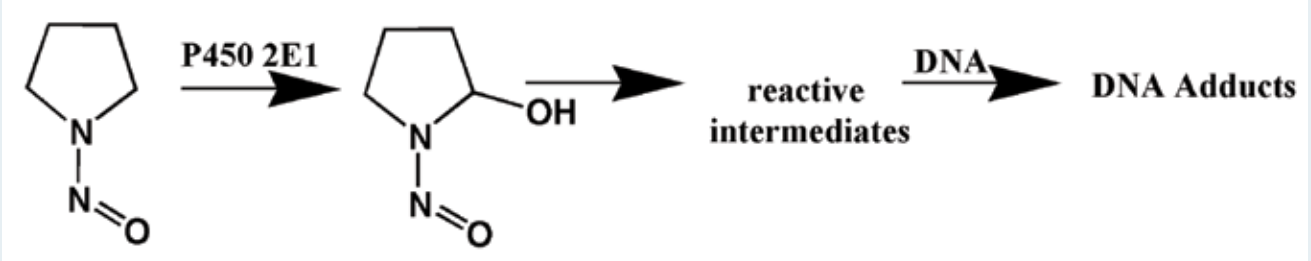

transferase in the microsomes with glucuronic acid to demonstrate a better detoxifying capacity for HLM than RLM using the ECL arrays. Taken together, lower genotoxicity and higher detoxication rates presented by HLM compared to RLM correlate with the much lower risk of tamoxifen for human liver cancer compared to rats.

The future vision for ECL toxicity arrays includes industrial and research applications to the screening of new environmental chemical and drug candidates for the formation of reactive intermediates, identifying the enzymes that produce them, and elucidating drug-drug interactions involving enzyme inhibition. For these types of arrays, we will need to include a more compete set of cyt P450 oxidations, bioconjugations, and multi-enzyme metabolic reactions in the arrays. In addition, higher throughput will be facilitated by ink jet spotting of the arrays, so that smaller spots and denser arrays can be fabricated. These developments are currently underway in our laboratories.

Acknowledgment

The authors thank the many student researchers, postdoctoral fellows and collaborators named in joint publications without whom the development of ECL toxicity arrays would not have been possible. The author's work described herein has been generously supported by U.S. PHS grant ES03154 from the National Institute of Environmental Health Sciences (NIEHS), NIH.

About the Author

James F. Rusling is Professor of Chemistry and Cell Biology at University of Connecticut. In 2009, he was an SFI Walton Research Fellow at the National University of Ireland at Galway. He is the 2009 recipient of the American Chemical Society Award in Electroanalytical Chemistry. Current research includes ECL arrays for toxicity prediction and electrochemical immunoarrays for cancer detection. He has authored nearly 300 research papers and several books. He also enjoys playing Irish and American folk music. He may be reached by e-mail at James.Rusling@uconn.edu.

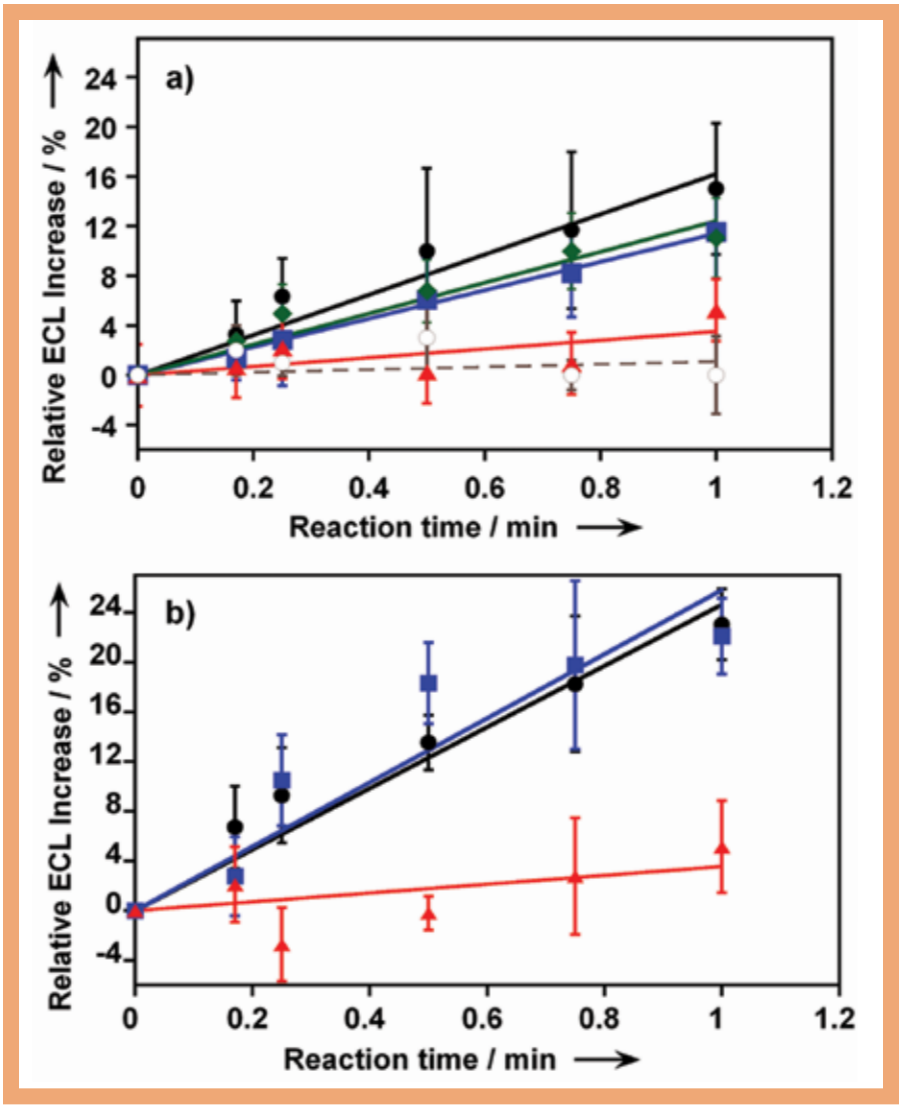

Fig. 5. *Percent ECL increase vs. reaction time for (a) RLM and (b) cyt P450 2E1 microsome (h2E1) arrays exposed to NPYR (black circles), NNK (blue squares), NPIP (green diamonds), or styrene (red triangles). Control (open circles, dash) in (a) is the ECL increase on a RLM array not exposed to any xenobiotic solution. Adapted with permission from Ref. 30, copyright 2008 American Chemical Society.*

References

1. M.Březina and P. Zuman, *Polarography in Medicine, Biochemistry, and Pharmacy*, Interscience, New York (1958).
2. G. Ramsay, Ed., *Commercial Biosensors*, Wiley, New York (1998).
3. J. B. Debad, E. N. Glezer, J. K. Leland, G. B. Sigal, and J. Wholstadter, in *Electrogenerated Chemiluminescence*, A. J. Bard, Ed., p. 359, Marcel Dekker, New York (2004).
4. (a) W. Miao and A. J. Bard, *Anal. Chem.* **76**, 5379 (2004); (b) X. Wang and D. R. Bobbitt, *Anal. Chim. Acta.*, **383**, 213 (1999); (c) H. P. Hendrichkson, P. Anderson, X. Wang, Z. Pittma, and D. R. Bobbitt, *Microchem. J.*, **65**, 189 (2000).
5. W. Miao, J. P. Choi, and A. J. Bard, *J. Am. Chem. Soc.*, **124**, 14478 (2002).
6. http://rochediagnostics.ca/lab/solutions/e2010.php
7. http://www.meso-scale.com/CatalogSystemWeb/WebRoot/technology/ecl.htm
8. L. Dennany, R. J. Forster, and J. F. Rusling, *J. Am. Chem. Soc.*, **125**, 5213 (2003).
9. A. E. F. Nasser, A. M. Kamel, and C. Clarimont, *Drug. Devel. Today*, **9**, 1055 (2004).
10. J. A. Kramer, J. E. Sagartz, and D. L. Morris, *Nature Rev. Drug Discov.*, **6**, 636 (2007).
11. J. T. Mayne, W. W. Ku, and S. P. Kennedy, *Curr. Op. Drug Disc. & Devel.*, **9**, 75 (2006).
12. D. Stoll, J. Bachmann, M. F. Templin, and T. O. Joos, *Drug Discov. Today: Targets*, **3**, 24 (2004).
13. J. F. Rusling, E. G. Hvastkovs, and J. B. Schenkman, *Curr. Opin. Drug Disc. & Devel.*, **10**, 67 (2007).
14. W. B. Jacoby, Ed., *Enzymatic Basis of Detoxification*, Vols. I and II, Academic, New York. (1980).

15. E. C. Friedberg, *Nature,* **421**, 436 (2003).
16. O. D. Scharer, *Angew. Chem. Int. Ed.,* **42,** 2946 (2003).
17. J. A. Bond, *CRC Crit. Rev. Toxicol.*, **19**, 227 (1989).
18. W. Pauwels, P. Vodiceka, M. Servi, K. Plna, H.Veulemans, and K. Hemminki, *Carcinogenisis*, **17**, 2673 (1996).
19. A. Umemoto, K. Komaki, Y. Monden, M. Suwa, Y. Kanno, M. Kitagawa, M. Suzuki, C.-X. Lin, Y. Ueyama, M. A. Momen, A. Ravindernath, and S. Shibutani, *Chem. Res. Toxicol.,* **14**, 1006 (2001).
20. M. Wang, E. J. McIntee, Y. Shi, G. Cheng, P. Upadhyaya, P. W. Villalta, and S. S. Hecht, *Chem. Res. Toxicol.,* **14**, 1435 (2001).
21. E. L. Cavalieri, E. G. Rogan, P. D. Devaneshan, P. Cremonesi, R. L. Cerny, M. L. Gross, and W. J. Bodell, *Biochemistry*, **29**, 4820 (1990).
22. J. B. Schenkman and H. Greim, Eds., Cytochrome P450, Springer-Verlag, Berlin (1993).
23. P. R. Ortiz de Montellano, Ed., *Cytochrome P450*, 3rd ed., Kluwer/ Plenum, New York (2005).
24. D. C. Liebler and F. P. Guengerich, *Nature Rev. Drug Discov.,* **4**, 410 (2005).
25. Y. Lvov, in *Protein Architecture: Interfacing Molecular Assemblies and Immobilization Biotechnology*, Y. Lvov and H. Mohwald, Eds., p. 125, Marcel Dekker, New York (2000).
26. J. F. Rusling, E. G. Hvastkovs, and J. B. Schenkman, in A. Nassar, P. F. Hollenburg, and J. Scatina, Eds., *Drug Metabolism Handbook***,** p. 307, Wiley, Hoboken, NJ, (2009).
27. M. So, E. G. Hvastkovs, J. B. Schenkman, and J. F. Rusling, *Biosens. Bioelectron.*, **23**, 492 (2007).
28. E. G. Hvastkovs, M. So, S. Krishnan, B. Bajrami, M. Tarun, I. Jansson, J. B. Schenkman, and J. F. Rusling, *Anal. Chem.*, **79**, 1897 (2007).
29. H. H. Thorp, *Topics Curr. Chem.*, **237**, 159 (2004).
30. S. Krishnan, B. Bajrami, E. G. Hvastkovs, D. Choudhary, J. B. Schenkman, and J. F. Rusling, *Anal Chem.*, **80**, 5279 (2008).
31. L. Zhao, S. Krishnan, Y. Zhang, J. B. Schenkman, and J. F. Rusling, *Chem. Res. Toxicology*, **22**, 341 (2009).